BNL--38477

DE86 015075

ANTIMATTER CLUSTERS FROM HADRONIZING QUARK-GLUON PLASMA

Ulrich Heinz

Physics Department
Brookhaven National Laboratory
Upton, NY 11973

ABSTRACT

We employ a realistic model for the phase transition between the color deconfining quark-gluon plasma phase and the color confining hadronic gas phase of nuclear matter to discuss the question how quarks and antiquarks hadronize in an expanding quark-gluon plasma. We pay particular attention to the problem associated with the latent heat and latent entropy set free in the hadronization process. Assuming a specific space-time scenario for the phase transition, we compute relative abundances of different hadronic particles and resonances produced during hadronization and show that in particular antinucleons and light antinuclei are enhanced above their equilibrium abundances in a hadron gas of similar density and temperature. We interpret this enhancement as a possible signature for the existence of a transient quark-gluon plasma phase in relativistic heavy-ion collisions which can complement the widely discussed strangeness signal. We point out, however, that detailed dynamical studies of the hadronization process are necessary in order to definitively settle questions about the quantitative yields.

Invited Lecture
NATO Advanced Summer Institute
PHYSICS OF STRONG FIELDS
June 1-14 1986
Maratea, Italy

This work was supported by the U. S. Department of Energy under contract DE-AC02-76CH00016.

ANTIMATTER CLUSTERS FROM HADRONIZING QUARK-GLUON PLASMA

Ulrich Heinz

Physics Department
Brookhaven National Laboratory
Upton, NY 11973

ABSTRACT

We employ a realistic model for the phase transition between the color deconfining quark-gluon plasma phase and the color confining hadronic gas phase of nuclear matter to discuss the question how quarks and antiquarks hadronize in an expanding quark-gluon plasma. We pay particular attention to the problem associated with the latent heat and latent entropy set free in the hadronization process. Assuming a specific space-time scenario for the phase transition, we compute relative abundances of different hadronic particles and resonances produced during hadronization and show that in particular antinucleons and light antinuclei are enhanced above their equilibrium abundances in a hadron gas of similar density and temperature. We interpret this enhancement as a possible signature for the existence of a transient quark-gluon plasma phase in relativistic heavy-ion collisions which can complement the widely discussed strangeness signal. We point out, however, that detailed dynamical studies of the hadronization process are necessary in order to definitively settle questions about the quantitative yields.

INTRODUCTION

After several years of intensive discussions whether in high energy collisions ($E_{lab} \geq 10$ GeV/n) between heavy nuclei (preferrably $A \geq 200$) a new state of nuclear matter, the quark-gluon plasma, would be formed and how one would experimentally detect it[1,2], the chase for the quark-gluon plasma is finally on. First experiments are scheduled for the Alternating Gradient Synchrotron (AGS) at Brookhaven National Laboratory and the SPS at CERN towards the end of this year and in early 1987, with projectile ions up to ^{32}S at 15 GeV/n at Brookhaven and up to ^{40}Ca at 60 and 225 GeV/n at CERN. Although the chances to produce a quark-gluon plasma in these first experiments are somewhat limited due to the small size of the projectile ions, we expect an abundance of valuable information on hadronic dynamics in relativistic nuclear collisions, thus filling in the big holes in our theoretical models for collisions in which this hadronic dynamics is modified by a transient quark-gluon plasma phase.

One of the biggest problems in identifying a quark-gluon plasma possibly formed in such a collision is the fact that the bulk of the emitted particles are color-singlet hadrons which are subject to the strong interaction and have very limited memory of the initial hot quark-gluon plasma phase. Rather, their momentum distribution etc. is determined mostly by the hadronization process in which the more or less thermally distributed quarks and gluons coalesce to form the mesons and (anti-) baryons which will final-

ly be detected. Due to its non-perturbative nature, this hadronization process is the most difficult step in a dynamical description of quark matter formation during heavy-ion collisions. On the other hand, its theoretical understanding may be essential in order to extract the necessary information from the spectrum of emitted hadrons that will allow us to prove that a quark-gluon plasma had been formed.

An important piece of information of that kind may be the chemical composition of the emitted hadrons, i.e. the abundance ratios between different species of mesons and (anti)baryons. It has been suggested that the abundance of strange particles[3] and antibaryons (including light antinuclei[4]) should be higher in collisions with a transient plasma phase than in purely hadronic collisions. The argument is based on a fast timescale for chemical equilibration of light antiquark and strage quark and antiquark densities at relatively high levels in the quark-gluon plasma phase (due to the large density of gluons and the small quark masses in this phase[5]), and on a destruction of chemical equilibrium by the hadronization process which allows to transfer the information on temperature and baryon density contained in those quark and antiquark abundances into the final hadron phase. Since the time before freeze-out of these hadrons into non-interacting, free-streaming particles is too short to reestablish chemical equilibrium on a hadronic level, the chemical composition of the detected hadrons should to some extent reflect the chemical composition in the transient quark-gluon plasma phase and should show striking deviations from what we expect in purely hadronic collisions by extrapolation from our experience from high energy p-p and p-A data.

I will concentrate in this lecture on antinucleon and antinucleus formation from hadronizing quark matter; the strange particle aspects will be discussed in a later lecture by J. Rafelski. Particles containing only antiquarks are in both cases selected because they are initially absent and therefore provide the best signal-to-noise ratio. Furthermore (this is particularly relevant for strange particles) once they are produced, the most dangerous thing that can happen to them is annihilation in a collision with a baryon; rescattering between pairs of antibaryons or antibaryons and mesons with flavor exchange are negligibly rare[3], whereas similar processes affect the baryons to a considerable extent leading to deviations in the final flavor distribution from the one originally produced during hadronization. Non-strange antibaryons and antinuclei have the advantage of being absolutely stable in vacuum and (except for the antineutron) negatively charged and are therefore easily detected. Furthermore, the light quark equilibration time in the original plasma phase is so short that saturation of the thermodynamic phase space limit can be reliably assumed for $\bar{q}$; for s and $\bar{s}$ this is generally not true unless the initial plasma temperature is larger than the strange quark mass of ~ 150 MeV, a condition which is hardly achievable in the experiments planned for the next few years. [Since for the available beam energies more or less complete stopping of the colliding nuclei within each other's volume is likely, a large fraction of the beam energy will be transformed into compression energy, leading to large baryon densities at moderate temperatures[6] ($\mu_q/T > 1$)]. At the higher beam energies planned for the future the temperature will increase, without appreciable increase in baryon density due to the onset of nuclear transparency[1,2]. Therefore, the ratio between the quark baryonic chemical potential and the temperature μ_q/T will decrease ($\mu_q/T \lesssim 1$) and the main argument for strange antibaryons over nonstrange antibaryons, namely that due to strangeness conservation $\bar{s}$ is not suppressed like $\bar{q}$ by a factor $e^{-\mu_q/T}$, will disappear.

However, there are also disadvantages of non-strange antibaryons: entropy conservation requires the production of many pions[7] in the hadronization process which drain a large fraction of $\bar{q}$'s from the interesting antibaryon channels. The same is only true to a much lesser degree for strange

particles because the lightest strange mesons, K and $\bar{K}$, are four times heavier than pions. Additionally, the annihilation cross section for antinucleons is considerably higher than for $\bar{\Lambda}, \bar{\Sigma}$ etc., making annihilation during the final hadron phase more likely for non-strange antibaryons. Finally, the vacuum itself outside the hadrons contains a condensate of light $q\bar{q}$ pairs which is responsible for chiral symmetry breakdown in the hadron phase[2]; the possible coupling of the light quarks from the plasma to this condensate during the hadronization process introduces a so far unavoidable uncertainty into all existing models for hadron production from a quark-gluon plasma.

THE MODEL EQUATION OF STATE

Before we can follow the quark and antiquarks through the phase transition defined by the hadronization process, we have to locate that phase transition and discuss its thermodynamic properties. We will here present a model in which the quark-gluon plasma is described as a weakly interacting gas of quarks and gluons subject to an external vacuum pressure given by the bag constant, while the hadron phase consists of a noninteracting gas mixture of baryonic and mesonic resonances with a finite proper volume. This is a highly sophisticated version of the so-called bag-model equation of state (EOS)[2] and yields, as we will see, results which are in good qualitative agreement with other models and with Monte Carlo results for numerical simulation of QCD on a lattice.

Calculations of the grand canonical potential for weakly interacting massless quarks and gluons from QCD in the 1-loop approximation yield[8]

$$-\Omega_Q = P_Q = \frac{8\pi^2}{45} T^4\left(1 - \frac{15\alpha_s}{4\pi}\right) + \sum_f \left\{\frac{7\pi^2}{60} T^4\left(1 - \frac{50\alpha_s}{21\pi}\right) + \left(\frac{\mu_f^2 T^2}{2} + \frac{\mu_f^4}{4\pi^2}\right)\left(1 - \frac{2\alpha_s}{\pi}\right)\right\} - B \quad (1)$$

where the sum is over quark flavors, and an external "bag" pressure from the outside true vacuum has been added. The quark chemical potentials μ_f contain a baryonic contribution μ_q and, in the case of strange quarks, an additional contribution $\tilde{\mu}_s$ due to the strangeness of these particles. Hence $\mu_u = \mu_d = \mu_q$ and $\mu_s = \mu_q + \tilde{\mu}_s$; for a system of zero net strangeness $\tilde{\mu}_s = -\mu_q$, and $\mu_s = 0$ in the quark-gluon plasma. From (1) all other thermodynamic variables, baryon density ρ_b, entropy density s, and energy density ε, are derived by straightforward differentiation:

$$\rho_{b,Q} = -\frac{1}{3}\frac{\partial \Omega_Q}{\partial \mu_q} ; \quad (2)$$

$$s_Q = -\frac{\partial \Omega_Q}{\partial T} ; \quad (3)$$

$$\varepsilon_Q = 3\mu_q \rho_{b,Q} + T s_Q - P_Q = 3P_Q + 4B . \quad (4)$$

In working out (4) one realizes that the outside vacuum pressure B also plays the role of a vacuum energy density in the quark-gluon plasma which is by an amount B higher than the energy density of the outside vacuum.

Although perturbation theory in QCD is problematic because a perturbative expansion of Ω_Q breaks down at order α_s^3 we include the 1-loop corrections to get a qualitative feeling of the effect of color interactions. We parametrize α_s by a QCD scale parameter Λ[4,5] which we vary over a range of values from 0 to 400 MeV, as stated when we show results.

For the hadron resonance gas we start from the expressions for a mixture of noninteracting fermions and bosons:

$$P_H = \sum_i P_i = \sum_i \frac{d_i}{6\pi^2} \int_{m_i}^{\infty} \frac{(E^2-m_i^2)^{3/2}\, dE}{e^{(E-\mu_i)/T} \pm 1} \quad ; \tag{5}$$

$$\rho_{b,H} = \sum_i b_i \rho_i = \sum_i \frac{b_i d_i}{2\pi^2} \int_{m_i}^{\infty} \frac{E(E^2-m_i^2)^{1/2}\, dE}{e^{(E-\mu_i)/T} \pm 1} \quad ; \tag{6}$$

$$\epsilon_H = \sum_i \epsilon_i = \sum_i \frac{d_i}{2\pi^2} \int_{m_i}^{\infty} \frac{E^2(E^2-m_i^2)^{1/2}\, dE}{e^{(E-\mu_i)/T} \pm 1} \quad ; \tag{7}$$

$$s_H = \left(\epsilon + P - \sum_i \mu_i \rho_i\right)_H / T \quad . \tag{8}$$

The sum goes over the spectrum of measured meson and baryon resonances, i.e., π, η, η', ρ, ω, K, K*, ϕ, ..., N, $\bar{N}$, Δ, $\bar{\Delta}$, N*, $\bar{N}$*, ... d_i is the spin-isospin degeneracy factor for species i. Initially we concentrate on non-strange particles, and we will discuss the effects of strangeness towards the end of this lecture. For non-strange particles only baryon number is conserved, and their chemical potential is proportional to the baryon number b_i carried by each particle of species i:

$$\mu_i = b_i \mu_b \qquad \sum_i \mu_i \rho_i = \mu_b \rho_b \quad . \tag{9}$$

THE HADRONIZATION PHASE TRANSITION

The phase coexistence line is determined by the three conditions

$$T_H = T_Q \text{ (thermal equilibrium)} \quad ; \tag{10a}$$

$$P_H = P_Q \text{ (mechanical equilibrium)} \quad ; \tag{10b}$$

$$\mu_b = 3\mu_q \text{ (chemical equilibrium)} \quad . \tag{10c}$$

The factor 3 in the last condition comes from the fact that quarks carry baryon number 1/3.

For small T,μ the pressure in the quark-gluon phase is smaller than in the hadronic phase, mainly because of the negative vacuum pressure -B. There the hadronic phase is stable. However, in general the quark-gluon plasma pressure increases with T and/or μ_q faster than the hadronic pressure. The reason is that many of the hadronic degrees of freedom are suppressed in the relevant temperature and density regime by their large masses, such that the quark-gluon phase has more effective degrees of freedom. These lead to a faster increase in pressure and, for a given μ_q, to a critical temperature $T_{cr}(\mu_q)$ at which $P_H = P_Q$, and the transition to the plasma phase takes place.

Note, however, that at extremely high T or μ where all the hadronic masses can be neglected, the hadronic phase as defined in (5)-(8) has the higher number of degrees of freedom and, if taken seriously, would again have the larger pressure and be stable (Fig. 1). This is due to the huge number of contributing resonances and their large spin-isospin degeneracy factors. Even for identical number of degrees of freedom, the pressure rises faster with increasing μ in the hadronic phase than in the quark-gluon phase, since in the plasma each quantum state can be filled by three times as many particles as in the hadronic gas, thus reducing the Pauli pressure.

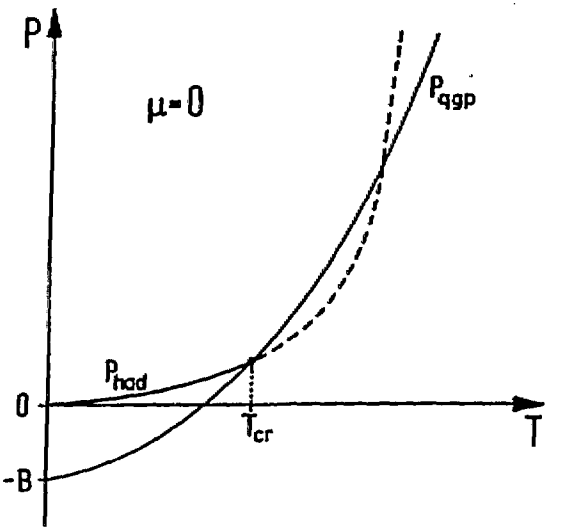

Fig. 1. Schematic behavior of the pressure in the hadronic resonance gas and in the quark-gluon plasma as a function of T at $\mu = 0$.

From the qualitative nature of Figure 1, it is conceivable that there exists a range of values for B and μ_q such that the two curves for P_H and P_Q never cross, and the hadronic phase never decays into the quark-gluon plasma. With the model (5)-(8) of pointlike, non-interacting hadronic resonances, this occurs actually for large values of μ_q and B (see Fig. 2).

This pathological behaviour is related to the one noted by Hagedorn[9]: in his statistical bootstrap model, he assumed that the spectrum of hadronic resonances continues towards higher masses with an exponentially increasing number of degrees of freedom, and this led to an increase of the pressure beyond limits at a finite, so-called 'limiting temperature' T_0 $[\sim O(m_\pi)]$. The origin for this singular behavior lies in the assumption of non-interacting pointlike hadrons which allows for the thermal production of arbitrarily many hadrons in a given volume and eventually leads to arbitarily high energy densities and pressures.

A simple remedy is provided by an inclusion of a finite proper volume for the hadrons[10-12]. This allows for a thermal production of more hadrons only until the fireball volume is completely filled with particles, and quenches the production of heavier hadrons which have larger proper volumes[10,11]. (Typical assumptions, which can be based on the MIT bag model for hadrons, take the proper volume of a hadron with mass m as $V_{had}=m/4B$[11]; or, in a system with energy density ε, a proper volume $V_{excl} = \varepsilon/4B$ is excluded from the available phase space for the thermally distributed hadrons[10]. In either case, B is a parameter which is usually taken to be identical with the QCD vacuum pressure discussed above.)

Within the bootstrap model[9,10] this correction for the proper volume is the only consistent one since, in the philosophy of the model, all other interactions between the hadrons are completely taken into account by choosing the correct hadronic mass spectrum. In our case where the hadronic mass spectrum is limited by our selection of resonances to be taken into account, further interactions should, in principle, be considered. The inclusion of interactions into a thermodynamic description is easy if the interactions are assumed to be local, i.e., they depend only on the particle densities[13].

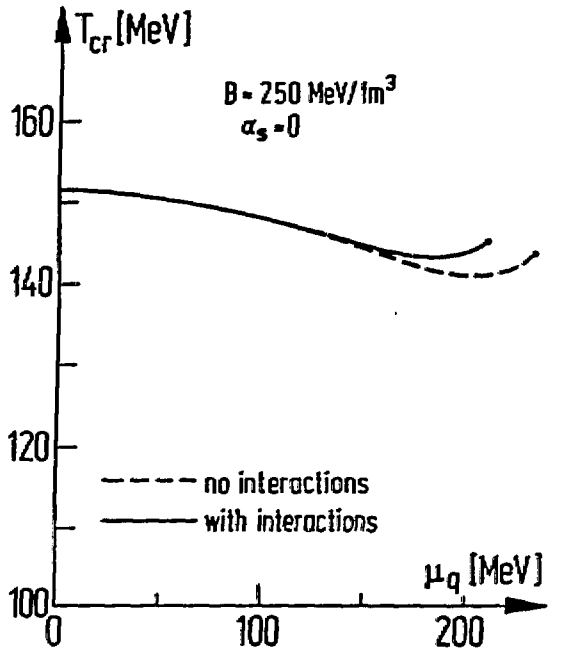

Fig. 2. The critical line for the transition from a gas of hadron resonances into a quark-gluon plasma. Dashed line: free, pointlike hadrons. Solid line: including a local interaction between the pointlike hadrons which is repulsive at large baryon densities.

A strong short-range repulsive interaction between the hadrons might be expected to have a similar effect of keeping the hadrons from getting too close to each other, thereby pushing even for pointlike hadrons the point, where particle densities, energy densities, and pressure become too big, to larger values for the temperature. We shall now discuss both these corrections to (5)-(8) with respect to their effect on the phase transition towards a quark-gluon plasma.

Density Dependent Interactions

If we simulate the short-range repulsion between hadrons by a vector exchange interaction and take the zero range limit such that the strength of the interaction depends only on the (baryon) density, its effect on the thermodynamics is easily included[4,13] by substituting in the thermal distribution functions:

$$\mu_i \longrightarrow \tilde{\mu}_i = \mu_i - W_i(\rho) \tag{11}$$

where $W_i(\rho)$ is the interaction felt by particles of species i. Working out the appropriate derivatives of the grand canonical potential Ω with the modification we find

$$\rho_b = \sum_i b_i \rho_i(\tilde{\mu}_i, T) \; ; \tag{12}$$

$$\varepsilon = \sum_i \rho_i W_i + \sum_i \varepsilon_i(\tilde{\mu}_i, T) \equiv \varepsilon_{int} + \varepsilon_{therm} \; ; \tag{13}$$

$$P = \sum_{i,j} \rho_i \rho_j \frac{\partial W_i}{\partial \rho_j} + \sum_i P_i(\tilde{\mu}_i, T) \equiv P_{comp} + P_{therm} \; ; \tag{14}$$

$$s = \left[\varepsilon - \sum_i \mu_i \rho_i + (P - P_{comp})\right]/T \; . \tag{15}$$

$\rho_i(\tilde{\mu}_i, T)$ etc. are given by integrals (5)-(8) with the substitution (11). The expressions for the interaction energy ε_{int} and P_{comp} simplify if $W_i(\rho)$ is assumed to be proportional to the baryon number b_i of species i:

$$W_i(\rho) = b_i W(\rho_b) \quad \text{with} \quad W(\rho_b) = -W(-\rho_b) \; . \tag{16}$$

Then $\sum_i \rho_i W_i = \rho_b W(\rho_b)$ and $\sum_{i,j} \rho_i \rho_j \, \partial W_i/\partial \rho_j = \rho_b^2 \, \partial W/\partial \rho_b$.

We tested the effect of this modification on the hadron gas equation of state with a form for $W(\rho_b)$ which reproduces saturation of nuclear matter at $\rho_0 = 0.17$ fm^{-3} with a binding energy of -16 MeV and a compressibility of 200 MeV, and which increases for large ρ_b linearly with the density. Such a repulsive interaction at high densities effectively raises the single particle energy levels, thereby reducing their occupation probability at a given temperature and reducing the thermal pressure. In view of Figure 1 and our attempts to force a crossing point with the quark-gluon plasma pressure curve also at high densities, this is a desired effect. However, the increase of $W(\rho_b)$ leads also to a strong compression pressure P_{comp} which is an undesirable effect because it more or less happens to cancel the reduction in P_{therm}. As shown in Figure 2, the net effect is negligible, and the system still avoids a phase transition at large enough baryon densities. Apparently we were not able to improve on this unphysical interaction because we still allowed the particles to get arbitrarily close to each other (even though at a tremendous cost in energy). Thus we did not actually reduce the allowed phase space to the extent that is required by the finite extension of the hadronic particles. As we will now see, such a van-der-Waals type correction for the hadronic proper volume is the essential ingredient into our thermodynamic description to obtain a transition to quark matter at low temperature and high baryon density.

Proper Volume Connection for Hadrons

There exist several suggestions in the literature as to how to take into account the finite proper volume of the particles within a thermodynamic framework. Without theoretical prejudice, we will use the prescription derived by Hagedorn[14] within the so-called pressure ensemble because it is extremely easy to implement: in the first step all thermodynamic quantities are calculated for pointlike hadrons using (5)-(8). The physical values for these quantities are obtained by finally applying a correction factor $1/(1+\varepsilon_H^{pt}/4B)$:

$$P_H = P_H^{pt} / \left\{1 + \varepsilon_H^{pt}/4B\right\} \; , \tag{17}$$

$$\varepsilon_H = \varepsilon_H^{pt} / \left\{1 + \varepsilon_H^{pt}/4B\right\} \; , \tag{18}$$

$$\rho_{b,H} = \rho_{b,H}^{pt} / \left\{1 + \varepsilon_H^{pt}/4B\right\} \; , \tag{19}$$

$$s_H = s_H^{pt} / \left\{1 + \varepsilon_H^{pt}/4B\right\} \; . \tag{20}$$

The parameter B here is taken to be identical with the bag pressure in the quark-gluon plasma EOS; 4B is the energy density inside an MIT bag, and

from (18) it is seen to form an upper limit to the energy density in the hadron gas. Before this limit is reached, we expect the phase transition to quark matter to have occurred. This is indeed borne out in the calculations[4], and the prescription (17)-(20) leads to a reasonable phase diagram for all baryon densities, shown in Figure 3a.

In Figure 3a-f we show for a specific value of B (B = 250 MeV/fm^3) the phase coexistence line and the behavior of the thermodynamic quantities

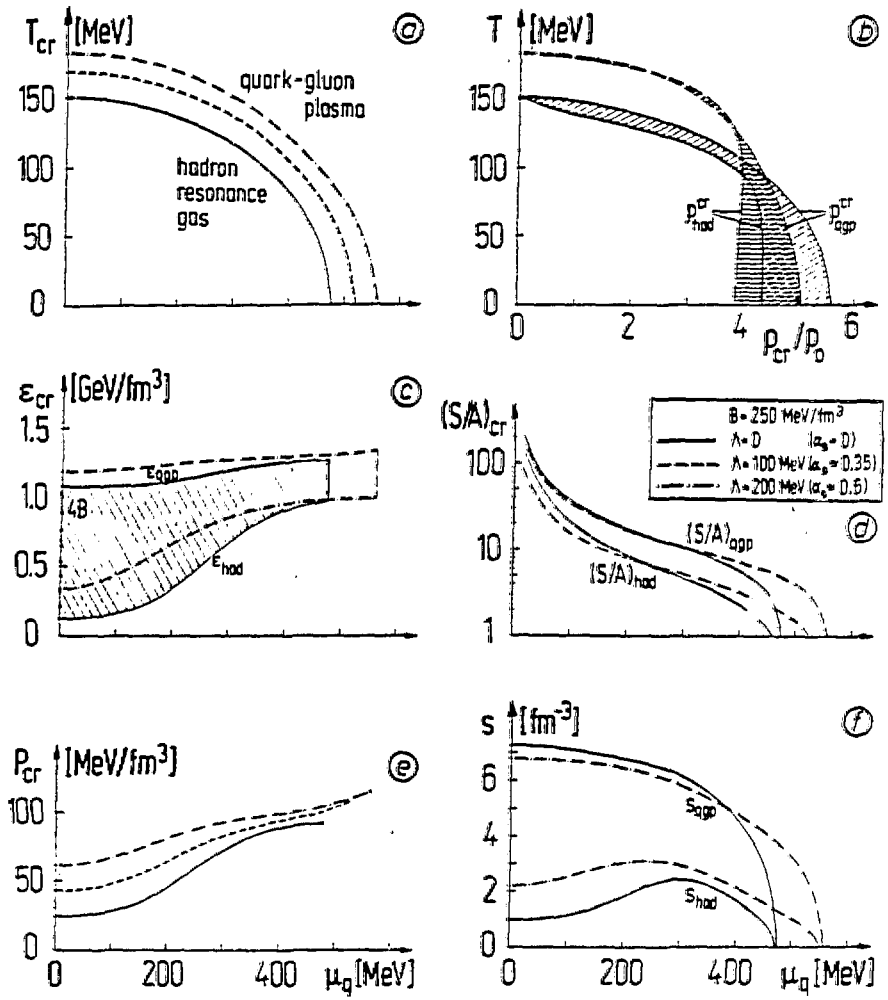

Fig. 3. a) The critical line (T,μ_q) for the hadronization transition, taking into account the proper volume of the hadrons in the resonance gas; b) baryon density; c) energy density; d) entropy per baryon; e) pressure; and f) entropy density along the critical line. Except in (b), all abscissae denote the chemical potential μ_q. Different style curves correspond to different values of α_s. The shaded region in (c) denotes the amount of latent heat. From Ref. 4.

along this critical line. Switching on the interactions in the quark-gluon plasma leads to an increase in the critical values for T and μ_q and to larger critical pressures and energy densities; this is due to the attractive nature of these interactions and the resulting reduction of the pressure in the quark-gluon plasma phase. Increasing the value of B has the same effect, and in both cases the point of pressure equilibrium (see Fig. 1) is shifted to higher values of T and μ_q.

Figure 3 shows that the phase transition in our model for hadronic matter is of first order, with large discontinuities in the energy density, entropy density, baryon density, and entropy per baryon. The latent heat (shaded region in Fig. 3c) is sizeable, namely of order 1 GeV/fm^3; the energy density increases by roughly an order of magnitude before the phase transition is completed at $\varepsilon \sim 1$-2 GeV/fm^3 (the exact value depends on the choice of B and A, but is more or less constant along the critical line). Similarly, there is a latent entropy of about a factor 3-5, i.e., the entropy density is considerably higher in the quark matter phase than in the hadron resonance gas (although not by a factor 12-15, as obtained with simpler and coarser models for the hadron gas[15]).

The first order nature of this phase transition is common to all existing models and basically due to the procedure of matching two different EOS, each of which is well motivated only safely away from the critical point. However, the amount of latent heat and latent entropy is similar to other models[1,2], and in particular Monte Carlo simulations of exact QCD on a lattice are also compatible with these numbers: although there a first order phase transition is only seen for a purely gluonic theory, and the inclusion of dynamical quarks tends to smear out the transition to the point where it may not be a phase transition in the mathematical sense any more[16], a similar increase in energy density and entropy density over a very small temperature interval is seen in these calculations[16,17]. Thus, for practical purposes our model will presumably be a very reasonable approximation to reality.

THE ENTROPY PROBLEM

Since the entropy discontinuity will play an important role in the dynamics of the hadronization process, let us study it in a little more detail. In Figure 4 we show the variation of the entropy density with the temperature for two values of the baryon chemical potential, $\mu_b = 0$ and $\mu_b = 750$ MeV. We plot $s(\hbar c/T)^3$ because at $\mu_b = 0$ for a gas of massless particles this would be a constant counting the number of degrees of freedom (as exemplified by the solid line labelled "free quark-gluon gas"). On the plasma side we included color interactions with $\alpha_s = 0.4$; note the strong decrease in s relative to the free gas limit. At $T = T_{cr}$ we see the entropy discontinuity across the phase transition. Below T_{cr} we split s into its contributions from different hadron resonances contained in the mixture. One sees that near T_{cr} the pions account for only about 30% of the entropy density, and that quantitatively the η, ρ, and ω mesons lead to a 100% correction, another 50% on top of that coming from the higher lying resonances. This trend starts already near T = 100 MeV, i.e., well below the phase transition, showing that a pure pion gas is quantitatively a poor approximation for the hadronic phase even at $\mu_b = 0$ and overestimates the entropy discontinuity by a factor of 3. Qualitatively the same conclusions hold at finite μ_b; the curve for the free quark-gluon gas increases in this plot at small T like 1/T due to the term $\sim \mu^2/T$ in the entropy density. Again the interactions in the plasma reduce s by nearly 50%. The bump below the phase transition is an artifact of the way we plot s (we use units of $(T/\hbar c)^3$) and just means that between T = 100 MeV and T_{cr} the entropy density does not increase as fast as T^3; this turns out to be mainly due to the van der Waals correction for the proper hadron volume which begins to suppress

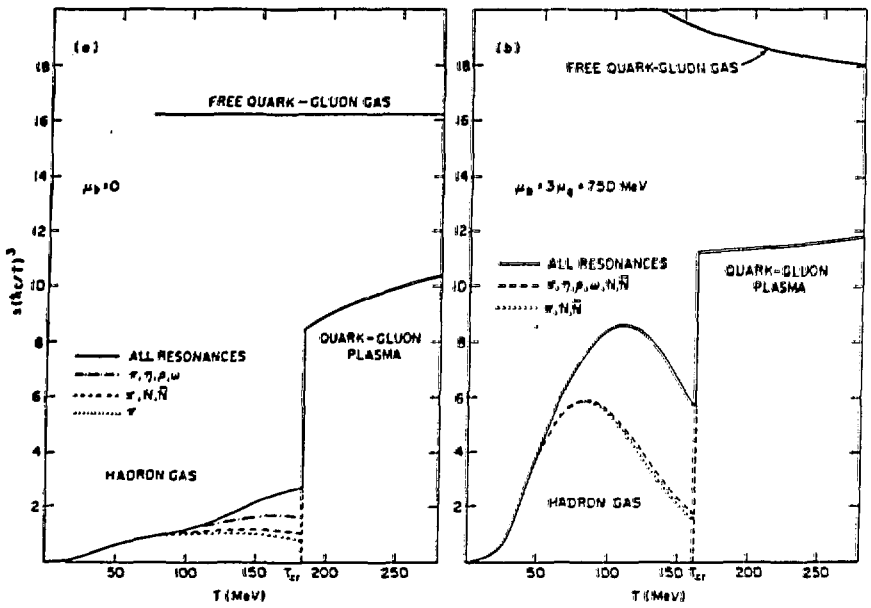

Fig. 4. The entropy density s in units of $(T/\hbar c)^3$ as a function of temperature. On the hadron gas side of the phase transition, contributions from different sets of hadronic resonances have been singled out in order to demonstrate their relative importance. On the plasma side, the limit for a non-interacting quark-gluon gas is indicated for comparison. The QCD scale parameter was chosen as Λ = 200 MeV, leading to $\alpha_s \approx 0.4$ just above the phase transition. The parameters are: B = 250 MeV/fm^3; μ_q = 0 (Fig. 3a) and μ_q = 250 MeV (Fig. 3b).

the effective degrees of freedom. Still it is obvious that the presence of all the high lying resonances leads to a big contribution to s already well below the phase transition. For a quantitative description it is therefore essential to take them into account.

Since the phase transition in our model is of first order, hadronization (if it happens locally on a fast time scale) will proceed through a mixed phase where hadron gas and plasma coexist inside the collision zone. It has been argued[15] that the lifetime of this mixed phase is determined by the entropy discontinuity because the entropy flux through the surface separating plasma from hadron gas is limited. Model calculations with a massless pion gas approximating the hadronic phase give rise to very long mixed phase lifetimes[15] ($\gtrsim$20 fm/c); however, our calculations show that the presence of hadronic resonances reduces the entropy discontinuity by a factor of 3 or 4, thereby also reducing the above predictions for the lifetime of the mixed hadronization phase. This conclusion is not easily avoided by invoking a deflagration shock wave[18] from which the hadronic matter emerges at a temperature $T < T_{cr}$, where the pion gas approximation becomes increasingly better; for it to be sufficient, the temperature would need to jump across the shock front by about 70 MeV.

While the discontinuity of the entropy density thus affects the dynamics of the hadronization process, there is also a problem with conservation of overall entropy[3,7,19]. Obviously the total entropy must not decrease during hadronization. To illustrate the implications of this constraint,

let us consider the case $\mu_q = 0$. The total entropy of the quark-gluon plasma is then given by

$$S = 4(N_q + N_{\bar{q}} + N_g) , \tag{21}$$

since for massless fermions $S/N = 4.202$ and for massless bosons $S/N = 3.602$. At the critical temperature $N_g \sim 2N_q = 2N_{\bar{q}}$, hence

$$S_Q = 8(N_q + N_{\bar{q}}) . \tag{22}$$

If we approximate the hadron phase by a massless pion gas (only for illustration), we find

$$S_H = 4N_\pi = 2(\tilde{N}_q + \tilde{N}_{\bar{q}}) \tag{23}$$

where $\tilde{N}_q$ and $\tilde{N}_{\bar{q}}$ are the total number of valence quarks and valence antiquarks in the hadron gas. Obviously, the condition $S_H \geq S_Q$ requires the number of valence quarks in the hadronic phase to be considerable larger than the number of quarks in the plasma; otherwise it is not possible to absorb all the entropy present in the gluons that disappear during hadronization from the excitation spectrum. Koch, Müller, and Rafelski therefore suggested[3,19] that during hadronization gluons fragment into additional quark-antiquark pairs, thereby saving the entropy balance. Both the thermally excited quarks and those from gluon fragmentation then recombine into mesons and baryons and determine the chemical composition of the hadron gas.

THE HADRONIZATION PROCESS - ANTINUCLEON AND ANTINUCLEI ABUNDANCES

In Figure 5 we show the light quark and antiquark densities along the critical line of phase coexistence. The hadron gas curve is obtained by counting the valence quarks and antiquarks contained in the hadrons. It is seen that the quark and antiquark density is about a factor 3 or so larger when the phase transition to quark matter is completed than what it was when the first hadrons started to dissolve. On the way back, i.e., during hadronization, additional $q\bar{q}$ production from gluon fragmentation will tend to increase that factor. On the other hand, the hadronization process will also involve some increase in volume of the system, tending to reduce the quark densities. The precise evolution governed by the counterplay of these two effects contributes the problem of hadronization dynamics and will determine the chemical composition of the hadron resonance mixture emerging from the hadronization process. This question can by no means be considered solved at the present time, but there exist several theoretical attempts, one of which we are now going to discuss in some detail. [Note that in Figure 5 the curves for the s and $\bar{s}$ densities would start at $\mu_q = 0$ about a factor 3 below the curves shown for light quarks, and due to the vanishing chemical potential of the strange quarks in the plasma phase and its relative smallness in the hadron phase[20], their values will stay nearly constant until the phase transition temperature begins to drop drastically near $\mu_q = 300$ MeV. On the other hand, the curves in Figure 5 for the light antiquark densities do not drop by a factor of 3 before $\mu_q \geq 150$-200 MeV. Only then (i.e., for $\mu_q/T \geq 1$) strange antiquarks become more abundant than light antiquarks and there will be an appreciably higher chance to form, say, strange rather than non-strange antibaryons. It is not clear without a complete dynamical calculation under which conditions regions with $\mu_q/T > 1$ will be formed in a heavy-ion collision. To get some idea one may look at Figure 4 of Ref. 6; even in the hydrodynamic approximation, i.e., assuming complete stopping of the nuclei, μ_q/T does not appreciably increase with the collision energy but appears to be limited by $\mu_q/T \sim 2$-3.]

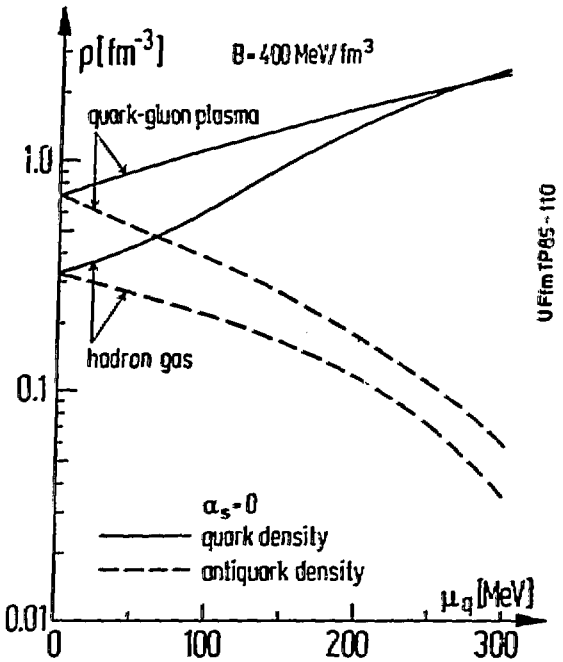

Fig. 5. The critical values for the quark and antiquark densities along the phase transition line shown in Fig. 3. In the hadron gas the (anti)quark density is computed by counting valence (anti)quarks. B = 400 MeV/fm^3.

Let us start by assuming that the plasma, once formed, has expanded and cooled down again to a point on the critical line $T(\mu_q)$ where hadronization begins. At this point we can compute the quark and antiquark densities ρ_q and $\rho_{\bar{q}}$ (see Fig. 5). After hadronization these quarks and antiquarks have to end up in hadrons; this will occur by recombination, e.g., of 3 quarks going into a baryon, a quark and an antiquark forming a meson, or 12 antiquarks forming an $\bar{\alpha}$-nucleus. Let us assume that these processes happen fast, and that at each point there is chemical equilibrium between the quarks and antiquarks on the one side and the hadrons forming from them on the other side. Then, if we define Lagrange multipliers ("chemical potentials") ν, $\bar{\nu}$ to keep count of the average quark and antiquark numbers (in the grand canonical sense), the chemical potential of the hadrons will be related to ν and $\bar{\nu}$ by their valence quark contents:

$$\begin{aligned}
&\mu_\pi = \nu + \bar{\nu} = \mu_\rho = \mu_\omega = \mu_\eta = \ldots && \text{(mesons)}\\
&\mu_1 = 3\nu = \mu_\Delta = \mu_{N^*} = \ldots && \text{(baryons)}\\
&\mu_d = 6\nu && \text{(deuteron)}\\
&\mu_{\bar{N}} = 3\bar{\nu} = \mu_{\bar{\Delta}} = \mu_{\bar{N}^*} = \ldots && \text{(antibaryons)}\\
&\mu_{\bar{d}} = 6\bar{\nu} && \text{(antideuteron)}
\end{aligned} \qquad (24)$$

etc. These equations are easily generalized, if strange quarks are to be included. Note that although all baryons, all mesons, etc. have the same

chemical potential, their production rates during hadronization will decrease with increasing resonance mass due to the mass term in the thermal distribution functions. This is in contrast to the recombination + fragmentation model by Koch, Müller, and Rafelski[3,19] where the number of produced hadrons of a given species is given only by a combinatorial factor depending on its valence quark content, and the mass difference, say between an N and a Λ or a Λ and a Σ, does not enter.

Given the relations (24), all hadron densities $\rho_i\left(T,\mu_i(\nu,\bar{\nu})\right)$ can be determined as a function of ν and $\bar{\nu}$, and hence the hadronic valence quark content

$$\tilde{\rho}_q(\nu,\bar{\nu}) = \sum_i n_i \rho_i\left(T,\mu_i(\nu,\bar{\nu})\right) ;$$
$$\tilde{\rho}_{\bar{q}}(\nu,\bar{\nu}) = \sum_i \bar{n}_i \rho_i\left(T,\mu_i(\nu,\bar{\nu})\right) . \qquad (25)$$

Here n_i ($\bar{n}_i$) counts the number of valence quarks (antiquarks) in hadron i.

To determine ν and $\bar{\nu}$ we have to solve a set of matching conditions

$$\tilde{\rho}_q = \lambda\rho_q = (\rho_q + \Delta\rho_q) \cdot V_Q/V_H ;$$
$$\tilde{\rho}_{\bar{q}} = \bar{\lambda}\rho_{\bar{q}} = (\rho_{\bar{q}} + \Delta\rho_{\bar{q}}) \cdot V_Q/V_H . \qquad (26)$$

Here $\Delta\rho_q = \Delta\rho_{\bar{q}}$ is the number of additional quark-antiquark pairs per unit volume formed by gluon fragmentation in the hadronization process. This number is in principle determined by entropy conservation, but in practice one has to know the volume expansion factor V_Q/V_H and the (T,μ) trajectory the system takes during hadronization in order to evaluate it. The reason for this complication is[4] that the latent heat is set free during hadronization and, depending on how much of it is converted into collective hydrodynamic flow energy, leads to reheating. Subramanian et al.[21] worked out such a scenerio, assuming conversion at constant entropy per baryon, however without including the effects of gluon fragmentation. Considerable reheating is observed[21]. No complete dynamical hadronization calculation to account for <u>all</u> these effects has been performed until now.

Given these uncertainties and no way to resolve them without a complete dynamical model, we will here show results of a calculation where we assumed in (26) $\lambda = \bar{\lambda} = 1$. From entropy conservation one estimates that this corresponds to a volume expansion factor $V_H/V_Q \sim 2$ if the phase transition occurs at constant temperature. Possible reheating effects are neglected and have to be studied in the future.

In Figure 6 we show the results for the hadron densities emerging from hadronization at a value (T,μ_q) as they are obtained after solving the matching conditions (26) with $\lambda = \bar{\lambda} = 1$ for ν and $\bar{\nu}$ and inserting into (24) (solid lines). One sees that the solid lines (hadron densities from plasma hadronization) consistently lie above the dashed lines (equilibrium hadron densities), due to the need to absorb the larger density of quarks and antiquarks initially present in the plasma. The gain factors increas with the size of the hadronic cluster formed, because the gain factors pe quark essentially multiply. They are of order 3 or so for antibaryons and for anti-alpha nuclei they reach 2 orders of magnitude. Although the absolute yield drops exponentially with the cluster mass, the value for $\rho_{\bar{\alpha}}$ in Figure 6 at $\mu = 0$ for a fireball volume corresponding to, say, half a uranium nucleus translates into about 1 $\bar{\alpha}$-events per hour in the planned Relativistic Heavy Ion Collider if a luminosity of 10^{27} cm^{-2} sec^{-1} is assumed; without plasma formation one would have to wait for several days.

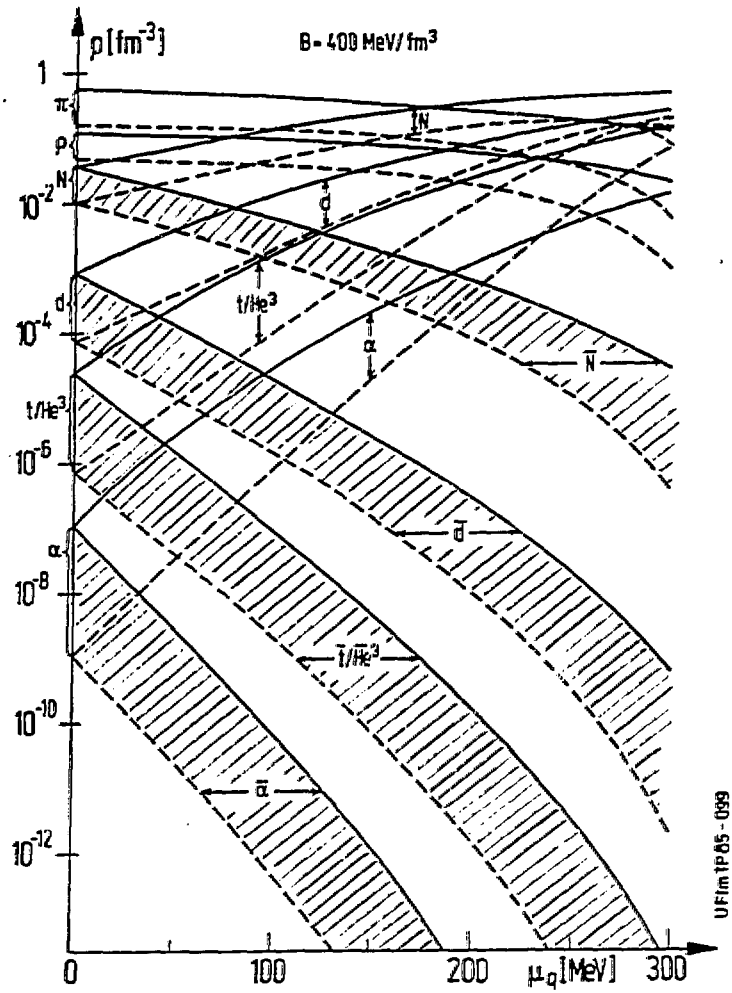

Fig. 6. Hadronic cluster densities as a function of the quark baryonic chemical potential in the initial quark-gluon plasma phase. Dashed curves denote the densities in an equilibrium hadron gas at the critical temperature corresponding to the given μ_q. Solid curves are the results obtained from a hadronization calculation which keeps the density of quarks and antiquarks fixed at the level of the original quark-gluon plasma (for details see text). B = 400 MeV/fm^3.

THE INFLUENCE OF STRANGE PARTICLES ON THE HADRONIZATION PROCESS

Before closing, we will now briefly look at the modifications that we will have to expect from the inclusion of strange particles. For a detailed account of strange hadrons from a quark-gluon plasma see Rafelski's talk in this volume. We will here concentrate on modifications to the critical quantities along the phase transition; a hadronization calculation for strange hadrons incorporating these changes has not yet been completed.

The grand canonical potential of the quark-gluon plasma now takes the form ($q,\bar{q}$ denotes light (massless) quarks):

$$-\Omega_Q = P_Q = P_{q\bar{q}g} + \frac{1}{\pi^2}\int_{m_s}^{\infty} dE(E^2-m_s^2)^{3/2}\left\{\frac{1}{e^{\beta(E+\mu_q+\tilde{\mu}_s)}+1} + \frac{1}{e^{\beta(E-\mu_q-\tilde{\mu}_s)}+1}\right\} . \quad (27)$$

The sum over hadrons in the hadron resonance gas expressions is extended to include K^-, K^0, $\bar{K}^0$, Λ, $\bar{\Lambda}$, ϕ ... . The strange hadron chemical potentials in chemical equilibrium are determined as before; e.g. $\mu_{K^-} = \mu_q+\tilde{\mu}_s+\mu_{\bar{q}} = \tilde{\mu}_s$, $\mu_\Lambda = 3\mu_q+\tilde{\mu}_s$, $\mu_\phi = 0$, etc. Imposing the conservation of total strangeness at its zero initial value $S = 0$ leads to $\tilde{\mu}_s = -\mu_q$ in the plasma phase; however, in the hadron gas this relationship has to be violated[20] for nonvanishing μ_q: due to the suppression of light antiquarks at finite μ_q the dominant strange particles are Λ's, whereas the strange antiquarks are mostly contained in K^+ and K^0. It is easily seen that the assumption $\tilde{\mu}_s = -\mu_q$ for the valence quarks does not lead to a system with zero strangeness, due to the chemical potential of the additional light quarks in the Λ's. Therefore,

$$\tilde{\mu}_{sH} \neq \tilde{\mu}_{sQ} = -\mu_q . \quad (28)$$

Hence, we now have two non-identical critical lines (T_{cr},μ_q) and $(T_{cr},\tilde{\mu}_{sH})$ shown in Figure 7. The difference between the two curves is a measure for the discontinuity of $\tilde{\mu}_s$ across the phase transition. They can be considered as different projections of one critical line in the 3-dimensional space spanned by $(T,\mu_q,\tilde{\mu}_{sH})$. It is seen that the strange particles reduce the critical temperature by a few percent, due to a relative increase of the pressure in the plasma phase over the hadron phase (where strange quarks have less influence owing to their larger effective mass).

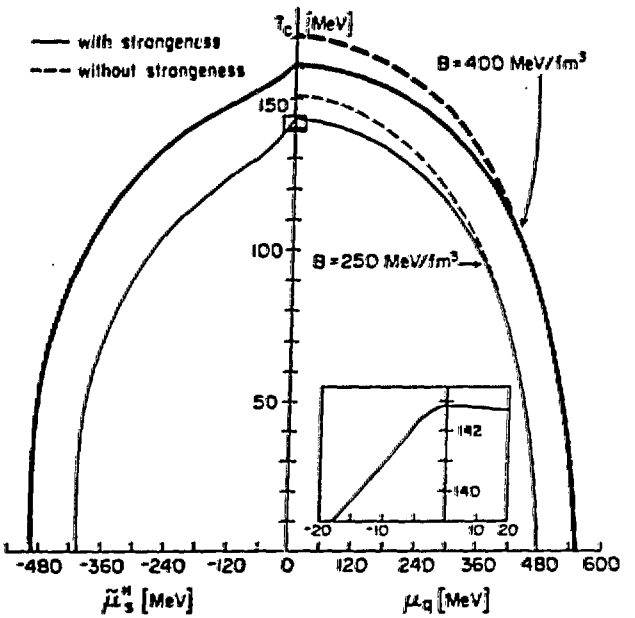

Fig 7. Projections of the critical line $(T,\mu_q,\tilde{\mu}_{sH})$ on the (T,μ_q) and $(T,\tilde{\mu}_{sH})$ planes. The dashed lines are for comparison and show the critical line (T,μ_q) in absence of strange particles. Two different bag constants have been chosen as indicated. Note the reduction in the critical temperature by about 5%. The inset shows that both curves are smooth near $\mu = 0$. From Ref. 20.

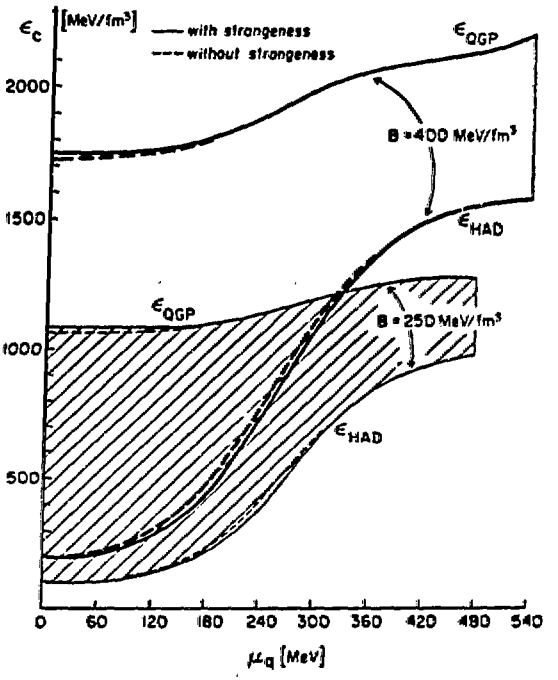

Fig. 8. The energy density along the critical line of Fig. 7, parametrized by μ_q. The curve labelled ϵ_{had} (ϵ_{QGP}) denotes its value on the hadron gas (quark-gluon plasma) side of the phase transition. The shaded area demonstrates the large amount of latent heat set free in the hadronization process. Solid (dashed) lines incorporate (omit) strange particles. Plotted against μ_q, the influence of strangeness on the critical energy densities is minimal. From Ref. 20.

It is important to note that this change in T_{cr} has virtually no effect on the values for the critical pressure and critical energy density (Fig. 8). The influence of strange particles just leads to a shift of the crossing point between the two pressure curves in Figure 1 to a smaller value of T_{cr}, but at a nearly unchanged value for P_{cr}.

CLOSING REMARKS

In this lecture I presented a model for the hadronization phase transition which is sophisticated enough to allow an analysis of the chemical composition of the hadron gas emerging from a hadronizing quark-gluon plasma. The phase transition was obtained by matching the equation of state for a weakly interacting quark-gluon plasma with a gas of hadronic resonances taken from the particle data tables. We have seen that accounting for the proper volume of the hadrons in the hadron gas is an essential ingredient to obtain a reasonable phase diagram also at large baryon densities, whereas the inclusion of longer range interactions between the hadrons does not qualitatively affect the phase transition.

In our model the phase transition is of first order and exhibits a large latent heat and latent entropy. Although the actual transition in

nature may not be of first order, we discussed that even there the energy and entropy densities show strong variations over a small temperature interval, and that our model will be a good qualitative approximation. We reviewed the argument by Koch, Müller, and Rafelski that during hadronization the total entropy balance can only be satisfied if additional quark-antiquark pairs are created in the hadronization process.

The hadronization itself is a difficult problem for which, so far, no microscopy model exists. We discussed here a statistical model which is based on chemical equilibrium between quarks and hadrons during the clustering process. Rafelski in his lecture discusses a clustering model mainly based on combinatorial considerations. I believe that these two models are complementary, and reality has to lie somewhere in between. Both models are, so far, incomplete as no full self-consistent dynamical study has been performed in which the respective hadronization model is coupled to a hydrodynamical evolution which correctly treats the energy and entropy balance. In particular, the volume expansion factors during hadronization are uncertain and can only be bounded between extremes. Still, both models for the clustering process agree qualitatively in their prediction that antibaryons and light antinuclei should be enhanced in hadronization of a quark-gluon plasma over their hadronic equilibrium values. Rafelski will argue that this enhancement works even better for strange antibaryons ($\Lambda,\Sigma,\ldots$), particularly at large μ_b, but I have given arguments that looking for nonstrange antibaryons may be easier experimentally and nearly as promising quantitatively. For both strange and nonstrange particles, generally the gain factors increase while the yields decrease with increasing size of the observed cluster.

Still, the quantitative predictions are uncertain, and it cannot be stressed often enough that the questions about actual yields to be expected in experiment cannot be reliably settled without a full dynamical calculation. This should be (and is for me) the highest priority project in the context of using strange and antimatter as a signature for quark-gluon plasma formation.

ACKNOWLEDGEMENT

I would like to thank my collaborators W. Greiner, K.S. Lee, M. Rhoades-Brown, H. Stöcker, and P.R. Subramanian, who had an essential part in obtaining the results I presented in this lecture. Interesting and clarifying discussions with P. Koch and B. Müller are gratefully acknowledged.

This work was supported by the U. S. Department of Energy under contract DE-AC02-76CH00016.

REFERENCES

1. "Statistical Mechanics of Quarks and Hadrons", H. Satz (ed.), North Holland, Amsterdam (1981);
   "Quark Matter '83", T.W. Ludlam and H.E. Wegner (eds.), Nucl.Phys.A 418 (1984);
   "Quark Matter '84", K. Kajantie (ed.), Lecture Notes in Physics 221, Springer, Heidelberg (1985);
   "Quark Matter '86", M. Gyulassy and L.S. Schroeder (eds.), to appear in Nucl.Phys.A (1986).
2. E.V. Shuryak, Phys.Rep. 61:71 (1980) and 115:151 (1984);
   B. Müller, "The Physics of the Quark-Gluon Plasma", Lecture Notes in Physics 225, Springer, Heidelberg (1985);
   J. Cleymans, R.V. Gavai, and E. Suhonen, Phys.Rep. 130:217 (1986).
3. J. Rafelski, Nucl.Phys.A 418:215c (1984);
   P. Koch, B. Müller, and J. Rafelski, Phys.Rep. (1986), in print.

4. U. Heinz, P.R. Subramanian, and W. Greiner, Z.Phys.A 318:247 (1984); U. Heinz, P.R. Subramanian, H. Stöcker, and W. Greiner, J.Phys.G (1986), in print.
5. J. Rafelski and B. Müller, Phys.Rev.Lett. 48:1066 (1982).
6. H. Stöcker, Nucl.Phys.A 418:587c (1984).
7. N.K. Glendenning and J. Rafelski, Phys.Rev.C 31:823 (1985).
8. J. Kapusta, Nucl.Phys.B 148:461 (1979).
9. R. Hagedorn, Suppl. Nuovo. Cimento 3:147 (1965); 6:311 (1968).
10. R. Hagedorn and J. Rafelski, in Ref. 1, p. 237 and 253.
11. J. Kapusta, Phys. Rev. D 23:2444 (1981).
12. P.R. Subramanian, L.P. Csernai, H. Stöcker, J.A. Maruhn, W. Greiner, and H. Kruse, J. Phys. G 7:L241 (1981).
13. U. Heinz, W. Greiner, and W. Scheid, J. Phys. G 5:1383 (1979).
14. R. Hagedorn, Z. Phys. C 17:265 (1983).
15. B. Friman, K. Kajantie, and P.V. Ruuskanen, Nucl. Phys. B 266:468 (1986); H. von Gersdorff, L. McLerran, M. Kataja, and P.V. Ruuskanen, Phys. Rev. D (1986) in print.
16. R.V. Gavai and F. Karsch, Nucl. Phys. B 261:273 (1985).
17. H. Satz, Ann. Rev. Nucl. Part. Sci. 35:245 (1985).
18. L. van Hove, Z. Phys. C 21:93 (1983).
19. B. Müller, in "Quark Matter '86", Ref. 1.
20. K.S. Lee, M.J. Rhoades-Brown, and U. Heinz, Phys. Lett. B 174:123 (1986).
21. P.R. Subramanian, H. Stöcker, and W. Greiner, Phys. Lett. B 173:468 (1986).